The Journal of Chemical Physics

RESEARCH ARTICLE | SEPTEMBER 15 2023

On the electronic structure and spin–orbit coupling of BiB from photoelectron imaging of cryogenically-cooled BiB^- anion

Han-Wen Gao ; Hyun Wook Choi ; Jie Hui ; Wei-Jia Chen ; G. Stephen Kocheril ; Lai-Sheng Wang

J. Chem. Phys. 159, 114301 (2023)
https://doi.org/10.1063/5.0170325

The Journal of Chemical Physics ARTICLE pubs.aip.org/aip/jcp

On the electronic structure and spin–orbit coupling of BiB from photoelectron imaging of cryogenically-cooled BiB^- anion

Cite as: J. Chem. Phys. 159, 114301 (2023); doi: 10.1063/5.0170325
Submitted: 2 August 2023 • Accepted: 28 August 2023 •
Published Online: 15 September 2023

Han-Wen Gao, Hyun Wook Choi, Jie Hui, Wei-Jia Chen, G. Stephen Kocheril, and Lai-Sheng Wang[a)]

AFFILIATIONS

Department of Chemistry, Brown University, Providence, Rhode Island 02912, USA

[a)]Author to whom correspondence should be addressed: lai-sheng_wang@brown.edu

ABSTRACT

We report a study on the electronic structure and chemical bonding of the BiB molecule using high-resolution photoelectron imaging of cryogenically cooled BiB^- anion. By eliminating all the vibrational hot bands, we can resolve the complicated detachment transitions due to the open-shell nature of BiB and the strong spin–orbit coupling. The electron affinity of BiB is measured to be 2.010(1) eV. The ground state of BiB^- is determined to be $^2\Pi(3/2)$ with a $\sigma^2\pi^3$ valence electron configuration, while the ground state of BiB is found to be $^3\Sigma^-(0^+)$ with a $\sigma^2\pi^2$ electron configuration. Eight low-lying spin–orbit excited states [$^3\Sigma^-(1)$, $^1\Delta(2)$, $^1\Sigma^+(0^+)$, $^3\Pi(2)$, $^3\Pi(1)$, $^1\Pi(1)$], including two forbidden transitions, [$^3\Pi(0^-)$ and $^3\Pi(0^+)$], are observed for BiB as a result of electron detachment from the σ and π orbitals of BiB^-. The angular distribution information from the photoelectron imaging is found to be critical to distinguish detachment transitions from the σ or π orbital for the spectral assignment. This study provides a wealth of information about the low-lying electronic states and spin–orbit coupling of BiB, demonstrating the importance of cryogenic cooling for obtaining well-resolved photoelectron spectra for size-selected clusters produced from a laser vaporization cluster source.

I. INTRODUCTION

Group III–V compounds are important semiconductor materials. Borides of group V elements have drawn recent attention because of the discovery of ultrahigh thermal conductivity and high ambipolar mobility in the cubic boron arsenide.[1–3] Heavy group V borides are much less known, in particular, bismuth boride. While there have been theoretical calculations about its properties,[4–7] bulk bismuth boride has not been synthesized experimentally. Owing to the strong spin–orbit (SO) coupling, bismuth is important in topological insulators.[8] The bonding properties of Bi are expected to be different from those of its lighter group V congeners because the strong relativistic effects lead to a highly contracted 6*s* orbital in the Bi atom.[9] Theoretical calculations predicted that the electronic properties of bulk BiB would be different from other III–V semiconductors.[4–7] To understand the chemical bonding between bismuth and boron, we have investigated several Bi-containing boron clusters using photoelectron spectroscopy (PES) of size-selected anions.[10–13] Specifically, we have found the Bi–B single bond, the Bi=B double bond, and the Bi≡B triple bond.[10,11] In Bi-doped boron clusters, we have observed that they tend to form planar structures with the Bi atoms bonded to the periphery of boron clusters.[12,13] In all the Bi-containing boron clusters that we have investigated, the Bi 6*s* electrons essentially remain as a lone pair with little participation in chemical bonding. However, the simplest diatomic BiB molecule has eluded us because diatomic anions produced by our laser vaporization cluster source are usually vibrationally hot.[14,15] The vibrational hot bands can make the PES of even the seemingly simple diatomic systems challenging to assign if they are open-shell molecules with dense manifolds of electronic states.[16,17] We have recently demonstrated that coupling of a cryogenically cooled 3D Paul trap with a laser vaporization cluster source can produce vibrationally cold anions.[18–20] Here, we report a high-resolution photoelectron imaging (PEI) study of

cryogenically cooled BiB^- and compare the result with those from our magnetic-bottle PES apparatus, which cannot cool diatomic species effectively.

The photoelectron (PE) spectra of BiB^- are observed to display complicated detachment features because of the open-shell nature of BiB and the strong SO coupling that gives rise to a dense manifold of low-lying electronic states. We will show that the spectra obtained from the magnetic-bottle PES apparatus contain significant vibrational hot bands and cannot be definitively assigned. Other heavy isovalent group III–V diatomic species have been studied previously by PES,[21] but their spectral assignments were complicated by the presence of vibrational hot bands, making it challenging to distinguish electronic states from vibrational features in some cases. The heavy group IV metal dimers are isovalent with group III–V diatomics and have also been studied by PES.[22] Similarly, their assignments were complicated by the interference of vibrational hot bands and the multitude of SO-split electronic states.

In this paper, we report the first PEI study of vibrationally cold BiB^- using our newly built cryogenic 3D Paul trap coupled to a laser vaporization cluster source. Vibrational hot bands are completely eliminated in cryogenically cooled BiB^-, significantly simplifying the PE spectra. The high-resolution data along with the angular distribution information from PEI allow us to assign the observed spectral features relatively straightforwardly. The ground state of $Bi^{10}B^-$ is determined to be $^2\Pi(3/2)$ with a $\sigma^2\pi^3$ valence electron configuration and a vibrational frequency of 650(30) cm^{-1}, whereas that of neutral $Bi^{10}B$ is found to be $^3\Sigma^-(0^+)$ with a $\sigma^2\pi^2$ electron configuration and a vibrational frequency of 563(12) cm^{-1}. The electron affinity of BiB is measured to be 2.010(1) eV. A total of eight SO-split excited electronic states are observed due to electron detachment from the σ and π orbitals, including two forbidden transitions, $^3\Pi(0^-)$ and $^3\Pi(0^+)$. The wealth of electronic structure information obtained for BiB will be valuable to test theoretical methods aimed at treating relativistic effects and SO couplings.

II. EXPERIMENTAL METHODS

A. Magnetic-bottle PES

We conducted the PES experiments on BiB^- using two different experimental apparatus. A magnetic-bottle PES apparatus equipped with a laser-vaporization supersonic cluster source was used to take spectra at high photon energies. The details of the magnetic-bottle PES apparatus can be found elsewhere.[23,24] The BiB^- anion was produced by laser vaporization of a disk target made of mixed powders of bismuth and ^{10}B-enriched boron. The laser-induced plasma was cooled by a high-pressure He carrier gas seeded with 5% Ar. The clusters formed inside the nozzle were entrained by the carrier gas and cooled by supersonic expansion. After passing through a skimmer, the anions in the collimated beam were accelerated perpendicularly into a time-of-flight (TOF) mass spectrometer. The BiB^- dimer of current interest was selected and decelerated before being crossed by a detachment laser beam. Three different detachment laser wavelengths were used, including the second (532 nm, 2.331 eV), third (355 nm, 3.496 eV), and fourth harmonics (266 nm, 4.661 eV) of an Nd:YAG laser. Photoelectrons were collected with over 90% efficiency by the magnetic bottle and analyzed in a 3.5 m long electron TOF tube. Photoelectron kinetic energies were calibrated using the known transitions of the Bi^- atomic anion. The kinetic energy (E_k) resolution ($\Delta E_k/E_k$) of the magnetic bottle photoelectron analyzer was about 2.5%, that is, ~25 meV for electrons with 1 eV kinetic energy.

B. Photoelectron imaging of cryogenically cooled anions

High-resolution PES experiments were performed on a PEI apparatus newly equipped with a cryogenically cooled 3D Paul trap.[18–20] The PEI apparatus has been reported in detail previously.[25] The cluster source and laser vaporization target (prepared using isotopically enriched ^{10}B powder) are similar to that used on the magnetic-bottle PES apparatus presented above, except pure He was used as the carrier gas. After passing through a skimmer, the collimated cluster beam was sent directly into a 3D Paul trap cooled down to 4.2 K by a two-stage closed-cycle He refrigerator. The trapped anions were collisionally cooled by a mixed He/H_2 buffer gas (4:1 by volume) for 45 ms before being pulsed into the extraction region of a TOF mass spectrometer. The BiB^- anion was mass-selected and intercepted by a detachment laser in the interaction zone of a velocity map imaging (VMI) system. Photodetachment was performed using a YAG-pumped dye laser, as well as the second and third harmonic outputs from an Nd:YAG laser. Photoelectrons were projected onto a set of microchannel plates coupled with a phosphor screen and a charge-coupled-device camera. A typical experiment required about 100 000–300 000 laser shots to achieve reasonable signal-to-noise ratios. The VMI lens was calibrated using the PE images of Au^- and Bi^- at various photon energies. The PE images were analyzed by the maximum entropy method (MEVELER).[26] The resolution of the VMI system was ~0.6% for electrons with high kinetic energies and as low as 1.2 cm^{-1} for very slow electrons.[25]

Photoelectron angular distributions (PADs) are obtained from the PE images, which are characterized by the anisotropy parameter (β).[27] The differential cross-section of the photoelectrons can be expressed as

$$d\sigma/d\Omega = (\sigma_{Tot}/4\pi)[1 + \beta P_2(\cos\theta)], \quad (1)$$

where σ_{Tot} is the total cross-section, P_2 is the second-order Legendre polynomial, and θ is the angle of the photoelectron relative to the laser polarization. Thus, the PADs can be described by

$$I(\theta) \sim [1 + \beta P_2(\cos\theta)], \quad (2)$$

where β has a value ranging from −1 to 2. This model works well for single-photon ionization of randomly oriented molecules. According to the electric dipole selection rules, when an electron in an atom with angular momentum l is detached, the outgoing photoelectron wave must carry an angular momentum of $l \pm 1$. For example, if an electron is detached from an s atomic orbital ($l = 0$), the outgoing photoelectron will have $l = 1$ (pure p-wave) with $\beta = 2$. If an electron is detached from an atomic p orbital, the outgoing electron will carry $s + d$ partial waves with $\beta = -1$. It is non-trivial to interpret the β value for electron detachment from molecular orbitals (MOs), which are linear combinations of atomic orbitals. Nevertheless, the β value is still very useful to qualitatively assess the symmetries of the MOs involved in the photodetachment process[28] and provides additional information for spectral assignments.

III. RESULTS

A. PES from the magnetic-bottle apparatus

Figure 1 shows the PE spectra of BiB^- at three photon energies from the magnetic-bottle PES apparatus. Five detachment bands are observed in the highest photon energy spectrum at 266 nm [Fig. 1(c)]: two closely spaced bands (X and B) at around 2 eV and three bands at higher binding energies (F, G, and H). At 355 nm [Fig. 1(b)], vibrational fine features are resolved for band F (*f*) and band G (*g*), whereas band H is cut off. In addition to the better resolved X and B bands, a weak feature (hb2) is resolved on the lower binding energy side, which could be due to a vibrational hot band or vibrational feature to the X band. At 532 nm [Fig. 1(a)], a plethora of fine features are resolved. A weak peak (hb1) is observed at an even lower binding energy than hb2. In addition, peaks *a* and A are resolved between bands X and B. As shown previously, diatomic anions are particularly challenging to be cooled in our laser vaporization supersonic cluster source.[14,15] The spacing between peaks hb1 and hb2 and that between peaks hb2 and X are similar; however, they are larger than the spacing between peaks X and *a*. Thus, tentatively, hb1 and hb2 are two hot bands due to excitations of v = 1 and 2 of the BiB^- anion, whereas peak X is the 0-0 transition to the ground electronic state of BiB and peak *a* is due to vibrational excitation of the neutral BiB ground state. The separation of peak A from peak X is too large to be a vibrational feature and it likely represents a new electronic state of BiB. It is difficult to assign definitively the fine features resolved in the 532 nm spectrum or the higher binding energy detachment features in Fig. 1 without temperature-dependent studies or angular distributions to distinguish between vibrational features and electronic transitions.

B. PES from the high-resolution cryogenic PEI apparatus

Figure 2 displays a set of high-resolution PE images and spectra at 2.125, 2.210, and 2.331 eV photon energies around bands X and B for cryogenically-cooled BiB^-. We observe immediately that the hb1 and hb2 peaks disappear, confirming they are vibrational hot bands and yielding a vibrational frequency of 650 ± 30 cm^{-1} for the $Bi^{10}B^-$ anion from the data in Fig. 1(a). Peaks *a* and A are much better resolved. More importantly, several weak peaks are observed on the high binding energy side of band B [C, *d*, D, *e*, E in Fig. 2(c)] that are cut off in Fig. 1(a), and band B is resolved into two peaks (B and *c*). With the complete elimination of vibrational hot bands, the spectral features observed in Fig. 2 should be entirely due to low-lying electronic states of the BiB final states or vibrational features of the observed electronic states. Clear angular anisotropy is observed for each detachment transition, which will be shown to be crucial for the assignment of these complicated spectral features.

The X peak with a clear *s* + *d* wave angular distribution (Fig. 2 and Table I) should be the 0-0 transition to the ground electronic state of BiB and defines an accurate EA of 2.010 ± 0.001 eV for BiB from the spectrum in Fig. 2(a). A short vibrational progression is observed for the ground state transition, represented by peaks *a* and *b* [Fig. 2(b)]. A vibrational frequency of 563 cm^{-1} is measured for

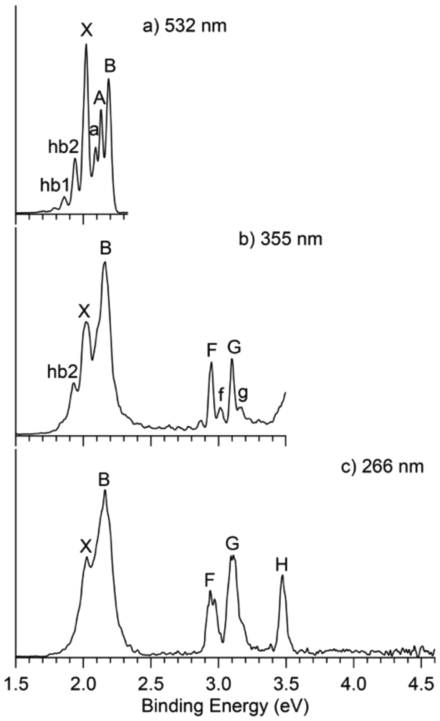

FIG. 1. The photoelectron spectra of $Bi^{10}B^-$ at (a) 532 nm (2.331 eV), (b) 355 nm (3.496 eV), and (c) 266 nm (4.661 eV) from the magnetic-bottle PES apparatus.

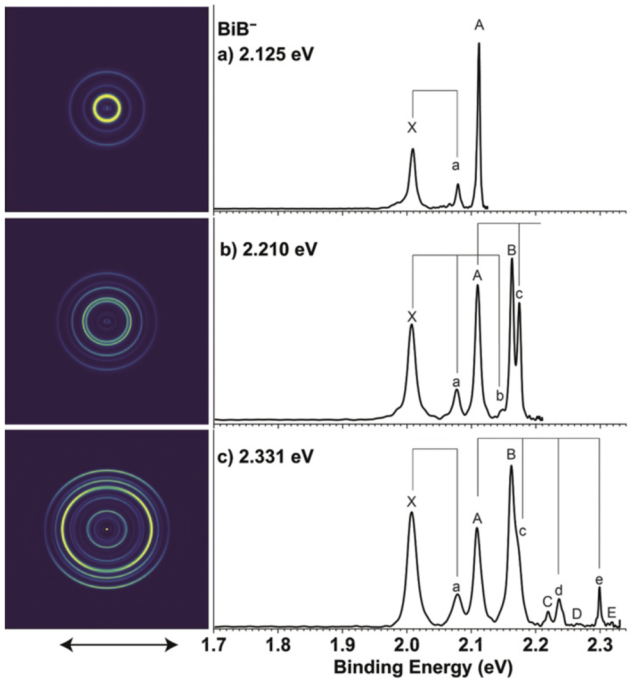

FIG. 2. Photoelectron images and spectra of cryogenically cooled $Bi^{10}B^-$ at (a) 583.46 nm (2.125 eV), (b) 561.01 nm (2.210 eV), and (c) 531.89 nm (2.331 eV). The double arrow below the image indicates the laser polarization.

TABLE I. The measured binding energies (BE) and assignments of the observed PES peaks of $Bi^{10}B^-$. The energy shift (ΔE) relative to peak X, the vibrational frequency of each electronic state, and the β value are also given.

Peak	Assignment	BE (eV)[a]	ΔE (eV)	Frequency (cm^{-1})[a]	β
X	$^3\Sigma^-(0)$	2.010(1)	0		−0.8
a	1_0^1	2.080(1)		563(12)	−0.7
b	1_0^2	2.149(2)			−0.5[b]
A	$^3\Sigma^-(1)$	2.112(1)	0.102		−0.7
c	1_0^1	2.175(1)			−0.4[b]
d	1_0^2	2.237(1)		504(8)	−0.6
e	1_0^3	2.299(1)			−0.3
B	$^3\Pi(2)$	2.163(1)	0.153		0.9
C	$^3\Pi(1)$	2.219(2)	0.209		0.4
D	$^3\Pi(0^-)$	2.269(5)	0.259		1.1
E	$^3\Pi(0^+)$	2.312(6)	0.302		1.0
F	$^1\Delta(2)$	2.947(2)	0.937		−0.4
f	1_0^1	3.012(1)[a]		516(20)	
G	$^1\Sigma^+(0)$	3.097(2)	1.087		−0.3
g	1_0^1	3.162(6)		524(20)	−0.3
H	$^1\Pi(1)$	3.475(1)	1.465		0.2

[a]The numbers in the parentheses represent the uncertainty in the last digit.
[b]These β values are obtained from the PE image taken at 2.210 eV, and all other values are from the PE image at 2.331 eV.

the ground state of $Bi^{10}B$ from the progression. Peak A, also with an $s + d$ wave angular distribution, should represent the origin of the first excited state of BiB, followed by a more extended vibrational progression (*c*, *d*, *e*), which yields a vibrational frequency of 504 cm^{-1}. Peak *e* seems to be slightly enhanced probably because it is close to the detachment threshold, suggesting that the *s*-partial wave is dominant according to the Wigner threshold law.[29] Peak B with a clear *p* wave angular distribution should be the second electronic excited state of BiB, but there is no discernible vibrational progression associated with this detachment channel. Peaks C, D, and E, which all have similar angular distributions as peak B but are not part of a vibrational progression, should be due to separate final electronic states.

Figure 3 displays the PE image and spectrum at 355 nm, showing bands F, G, and H. No new spectral features are resolved in comparison to the magnetic-bottle PES data in Fig. 1, except for the angular distribution information. Peaks F and G have $s + d$ type angular distributions, while peak H has a *p*-type angular distribution. The binding energies, vibrational frequencies, β parameters, and the assignment of all the observed spectral features are summarized in Table I. The binding energies measured from both apparatus agree with each other, but the more accurate data from the cryo-PEI experiment are given in Table I.

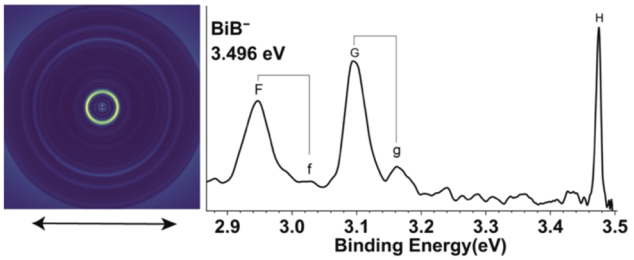

FIG. 3. The photoelectron image and spectrum of cryogenically cooled $Bi^{10}B^-$ at 355 nm (3.496 eV). The double arrow below the image indicates the laser polarization.

IV. DISCUSSION

A. General consideration of the electronic structure of BiB and BiB^-

There is no previous study on BiB^- or BiB and their electronic structure is not known, although several heavy group III–V isovalent diatomic species and heavy group-IV dimers have been studied using anion PES previously.[21,22] Because of the open-shell nature of these species compounded by vibrational hot bands, congested and complicated PES features were observed in the previous PES studies and the spectral assignments were challenging. The valence electron configuration of Bi is $6s^26p^3$ and that of B is $2s^22p^1$. The 6*s* and 2*s* orbitals combine to form a σ bonding orbital and a σ* antibonding orbital, which are fully occupied. The 6*p* and 2*p* orbitals combine to form a σ and a π bonding orbital and a σ* and a π* antibonding orbital. The four *p* electrons of BiB fill the two bonding orbitals to give either a $\sigma^2\pi^2$, $\sigma^1\pi^3$, or π^4 configuration. Omitting the filled σ and σ* MOs from the 6*s*/2*s* orbitals, we can have two possible electron configurations for BiB^-, $\sigma^2\pi^3$ or $\sigma^1\pi^4$, which can give rise to the following one-electron detachment channels to the neutral final states:

$$\sigma^2\pi^3(^2\Pi) \rightarrow \sigma^2\pi^2(^3\Sigma^-, {}^1\Delta, {}^1\Sigma^+), \quad (3)$$

$$\rightarrow \sigma^1\pi^3(^3\Pi_{0,1,2}, {}^1\Pi), \quad (4)$$

$$\sigma^1\pi^4(^2\Sigma^+) \rightarrow \sigma^1\pi^3(^3\Pi_{0,1,2}, {}^1\Pi), \quad (5)$$

$$\rightarrow \sigma^0\pi^4(^1\Sigma^+). \quad (6)$$

For heavy diatomic molecules, the **L**-**S** coupling is not a good description anymore, while the **J**-**J** coupling dominates. Under the **J**-**J** coupling scheme, the orbital angular momentum *L* and spin angular momentum *S* are no longer good quantum numbers; instead, the good quantum number is the total angular momentum *J* with $\boldsymbol{J} = \mathbf{L} + \mathbf{S}$. Since the **L**-**S** coupling scheme still provides an intuitive picture, we will keep the **L**-**S** label and give the *J* label in a parenthesis, e.g., $^{2S+1}L(J)$. Under the **J**-**J** coupling scheme, the final states from the photodetachment of BiB^- are expected as follows:

$$\sigma^2\pi^3(^2\Pi) \rightarrow \sigma^2\pi^2[^3\Sigma^-(0^+), {}^3\Sigma^-(1), {}^1\Delta(2), {}^1\Sigma^+(0)], \quad (7)$$

$$\rightarrow \sigma^1\pi^3[^3\Pi(2), {}^3\Pi(1), {}^3\Pi(0^-), {}^3\Pi(0^+), {}^1\Pi(1)], \quad (8)$$

$$\sigma^1\pi^4(^2\Sigma^+) \rightarrow \sigma^1\pi^3[^3\Pi(2), {}^3\Pi(1), {}^3\Pi(0^-), {}^3\Pi(0^+), {}^1\Pi(1)], \quad (9)$$

$$\rightarrow \sigma^0\pi^4[^1\Sigma^+(0^+)]. \quad (10)$$

The previous PES study on the isovalent III–V heavy diatomics indicates that transitions from the anion ground state to the triplet and singlet final states of the neutral are well separated into two manifolds.[21] The spectra of the triplet manifold are particularly complicated due to the SO coupling. All spectra exhibited a series of hot bands overlapping with multiple low-lying electronic states and their vibrational structures, making it challenging for the spectral assignment. The ground state of the AlP^-, GaP^-, InP^-, and $GaAs^-$ anions was determined to be $^2\Sigma^+$ with the $\sigma^1\pi^4$ electron configuration.[21] However, transitions from the low-lying excited $^2\Pi$ state of the anion were also observed. The ground state of the heavy isovalent group-IV diatomic anion ($SnPb^-$) was shown to be $^2\Pi(3/2)$ from the $\sigma^2\pi^3$ electron configuration.[22]

B. The ground electronic state of BiB^-: $^2\Pi(3/2)$ ($\sigma^2\pi^3$)

The key to assigning the complicated PE spectra of BiB^- is the elimination of the vibrational hot bands. The high-resolution PEI and the angular distribution information are also crucial. The difficulty to produce cold diatomic anions from the laser vaporization supersonic cluster source is shown vividly in the spectra of BiB^- obtained with the magnetic-bottle apparatus (Fig. 1). In this case, substantial populations of the v = 1 and 2 levels of BiB^- are observed. We have shown previously that for Au_2^-, which has a lower vibrational frequency, vibrational levels of the anion as high as v = 5 were observed, yielding a complicated PE spectrum for an otherwise single vibrational progression due to sequence bands from the hot bands.[15] In the high-resolution PE spectra obtained with the cryogenically cooled BiB^- (Fig. 2), all hot bands are eliminated. The complex spectral features are entirely due to the strong SO coupling in the open-shell BiB.

According to the β values measured from the PEI data (Table I), five electronic transitions (B, C, D, E, and H) exhibit *p*-type angular distributions (β > 0), corresponding to electron detachment from a σ orbital. If the ground state of the BiB^- anion is $^2\Sigma^+(\sigma^1\pi^4)$, electron detachment from the σ orbital would only give rise to a single detachment transition to the $^1\Sigma^+(\sigma^0\pi^4)$ final neutral state with a *p*-wave angular distribution [see detachment channel (10) above], clearly inconsistent with the experimental observation. On the other hand, detachment of a σ electron from the $\sigma^2\pi^3$ ($^2\Pi$) electron configuration would yield exactly five neutral electronic states under the **J**-**J** coupling scheme, $^3\Pi(2)$, $^3\Pi(1)$, $^3\Pi(0^-)$, $^3\Pi(0^+)$, and $^1\Pi(1)$, as shown in detachment channel (8) above. Thus, the ground state of the BiB^- anion should be $^2\Pi$ with the $\sigma^2\pi^3$ electron configuration. The SO coupling splits the $^2\Pi$ term into two components $^2\Pi(1/2)$ and $^2\Pi(3/2)$ with $^2\Pi(3/2)$ being lower in energy according to Hund's rules. Hence, the ground state term of BiB^- should be $^2\Pi(3/2)$. Furthermore, detaching an electron from the π orbital should give rise to four final states under **J**-**J** coupling, $^3\Sigma^-(0^+)$, $^3\Sigma^-(1)$, $^1\Sigma^+(0^+)$, and $^1\Delta(2)$, as shown in detachment channel (7) above, consistent with our experimental observation of four detachment transitions (X, A, F, and G) with *s* + *d* partial waves (β < 0, Table I).

C. Assignment of the PE spectra of BiB^-

With the determination of the ground state of BiB^-, the detailed assignment of the observed PES features is straightforward, as given in Table I. According to detachment channel (7), the removal of an electron from the highest occupied π bonding orbital gives rise to four **J**-**J**-coupled final states: $^3\Sigma^-(0^+)$, $^3\Sigma^-(1)$, $^1\Sigma^+(0^+)$, and $^1\Delta(2)$, which should display *s* + *d* angular distributions (β < 0). Thus, the ground state of BiB should be $^3\Sigma^-(0^+)$, corresponding to the X band, whereas band A should be assigned to the $^3\Sigma^-(1)$ state. Both PES bands display a vibrational progression with frequencies significantly lower than that of the BiB^- anion, consistent with the bonding nature of the π MO. The ordering of the $^3\Sigma^-(0^+)$ and $^3\Sigma^-(1)$ SO-split states is based on an off-diagonal SO interaction between the $^3\Sigma^-(0^+)$ and $^1\Sigma^+(0^+)$ states derived from the same electron configuration, thus stabilizing the $^3\Sigma^-(0^+)$ state.[30] Both bands F and G exhibit *s* + *d* angular distributions and they should correspond to the $^1\Sigma^+(0^+)$ and $^1\Delta(2)$ singlet states. According to Hund's rules, the $^1\Delta(2)$ state should be more stable and should be assigned to band F, while band G should be assigned to $^1\Sigma^+(0^+)$. A short vibrational progression is observed in both bands with vibrational frequencies significantly smaller than that of the anion, similar to that in bands X and A.

The five PES bands (B, C, D, E, and H) with *p* wave angular distributions should come from the detachment of a σ electron, described by detachment channel (8). According to Hund's rules, peaks B, C, D, and E should be assigned to $^3\Pi(2)$, $^3\Pi(1)$, $^3\Pi(0^-)$, and $^3\Pi(0^+)$, respectively, and peak H should be assigned to the $^1\Pi(1)$ singlet state. The degeneracy of the $^3\Pi(0^-)$ and $^3\Pi(0^+)$ states is lifted because the $^3\Pi(0^+)$ state can have SO interactions with the nearby lower-lying $^3\Sigma^-(0^+)$ state, pushing up the energy of the $^3\Pi(0^+)$ state.[30] It should be pointed out that the detachment transitions from the $^2\Pi(3/2)$ ground state of BiB^- to the $^3\Pi(0^-)$ and $^3\Pi(0^+)$ final states of neutral BiB are, in principle, forbidden, consistent with the very low detachment cross sections for these peaks [Fig. 2(c)]. However, the anisotropies of these two detachment features are unmistakable in the PE images. The definitive identification of these two weak transitions is entirely due to the elimination of vibrational hot bands and the angular anisotropy in the PE images. The observed $^3\Pi(0^-)$ and $^3\Pi(0^+)$ splitting of 0.043 eV is quite large, due to the contribution of the Bi $6p_z$ orbital to the σ MO of BiB, in comparison to the same splitting in the isovalent InP (0.014 eV) and GaAs (0.019 eV).[21]

D. The electronic structure and chemical bonding of BiB

Figure 4 schematically summarizes all the detachment transitions from the ground state of BiB^- to the ground and low-lying electronic states of BiB observed in this study. The electronic configurations (left) and the **J**-**J**-split levels (right) are given, as well as the measured excitation energies in eV and the vibrational frequencies in cm^{-1} were available. All possible transitions from the anion ground state of BiB^- [$^2\Pi(3/2)$] to the neutral BiB final states for one-electron detachment from the valence σ and π MOs are observed in this experiment, including the two forbidden transitions [$^3\Pi(0^-)$ and $^3\Pi(0^+)$]. The open-shell nature of BiB and the strong SO coupling give rise to the rather complicated spectral features, which can only be resolved and assigned with the elimination of vibrational hot bands and the high-resolution capability of PEI. The detailed electronic structure information provides valuable data to test computational methods to treat SO couplings and relativistic effects. This study proves the power of cryogenic cooling for high-resolution PES to investigate the electronic structure of size-selected clusters

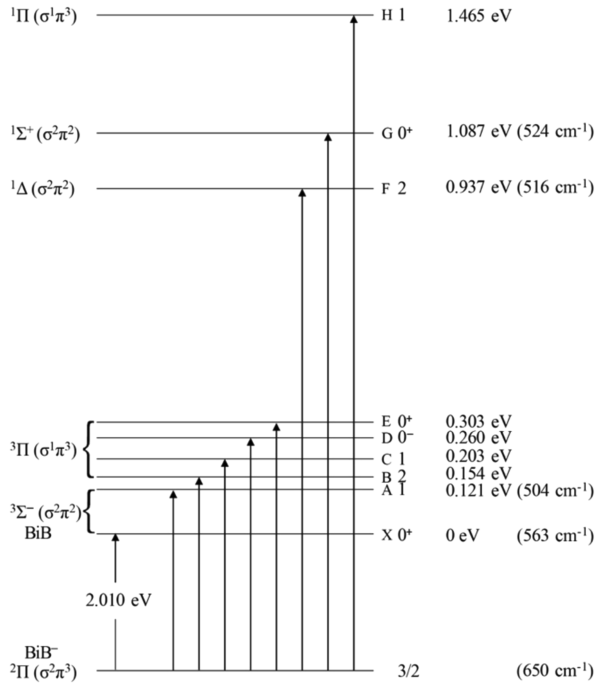

FIG. 4. The schematic energy level diagram for the observed detachment transitions from the ground state of BiB^- to the low-lying states of BiB. The electron configurations and electronic states of the anion and the neutral final states under **L-S** coupling, as well as the EA of BiB, are given on the left. The observed PES features, the electronic states under **J-J** coupling, the measured excitation energies of the neutral states, and vibrational frequencies (for $Bi^{10}B$), as well as the anion vibrational frequency, are given on the right.

produced from a laser vaporization cluster source, as also demonstrated by cryo-SEVI previously.[17,31,32]

The vibrational hot bands present in the spectra from the magnetic-bottle apparatus yield a vibrational frequency of 650 cm^{-1} for the ground state of the $Bi^{10}B^-$ anion [$^2\Pi(3/2)$]. The vibrational frequency for the ground state of neutral $Bi^{10}B$ [$^3\Sigma^-(0^+)$] is measured to be 563 cm^{-1}, significantly smaller than that of the anion, suggesting that the π MO is a strongly bonding orbital. The vibrational frequencies for the other electronic states [$^3\Sigma^-(1)$, $^1\Delta(2)$, $^1\Sigma^+(0^+)$] that are derived from the detachment of a π electron are all much smaller than that of the anion (Table I). Surprisingly, no vibrational structures are observed for any electronic states associated with the detachment of the σ bonding electron. This observation is consistent with the PES of other main group diatomic molecules, such as N_2 and CO, which display a much more extensive vibrational progression for the ionization of a π bonding electron than that for the ionization of a σ bonding electron.[33]

V. CONCLUSION

We have investigated the electronic structure and chemical bonding of BiB^- and BiB using a newly renovated high-resolution photoelectron imaging apparatus equipped with a cryogenically cooled 3D Paul trap. Because of the open-shell nature of both the BiB^- anion and neutral BiB and strong spin–orbit couplings, congested photoelectron spectra are observed with a dense manifold of spin–orbit split electronic transitions. It is shown that vibrational hot bands of BiB^- are completely eliminated in the cryogenic ion trap, allowing us to resolve all the low-lying electronic states of BiB below 1.5 eV excitation energy, including two forbidden transitions, $^3\Pi(0^-)$ and $^3\Pi(0^+)$. A wealth of low-lying electronic structure information is obtained for BiB, providing valuable experimental data to calibrate theoretical methods aimed at treating spin–orbit couplings and relativistic effects. This work demonstrates that we can trap and cool size-selected anions from a laser vaporization cluster source, opening the door for us to study cryogenically cooled clusters using high-resolution photoelectron imaging.

ACKNOWLEDGMENTS

This work was supported by the National Science Foundation (Grant No. CHE-2053541).

AUTHOR DECLARATIONS

Conflict of Interest

The authors have no conflicts to disclose.

Author Contributions

Han-Wen Gao: Conceptualization (equal); Data curation (lead); Formal analysis (lead); Writing – original draft (lead). **Hyun Wook Choi**: Conceptualization (equal); Data curation (supporting); Writing – original draft (supporting). **Jie Hui**: Data curation (supporting). **Wei-Jia Chen**: Data curation (supporting). **G. Stephen Kocheril**: Conceptualization (supporting). **Lai-Sheng Wang**: Conceptualization (lead); Formal analysis (supporting); Funding acquisition (lead); Writing – original draft (lead).

DATA AVAILABILITY

The data that support the findings of this study are available from the corresponding author upon reasonable request.

REFERENCES

[1] L. Lindsay, D. A. Broido, and T. L. Reinecke, Phys. Rev. Lett. **111**, 025901 (2013).
[2] F. Tian *et al.*, Science **361**, 582 (2018).
[3] J. Shin *et al.*, Science **377**, 437 (2022).
[4] D. Madouri and M. Ferhat, Phys. Status Solidi B **242**, 2856 (2005).
[5] S. Cui, W. Feng, H. Hu, Z. Feng, and Y. Wang, Comput. Mater. Sci. **47**, 968 (2010).
[6] B. G. Yalcin, S. Bagci, M. Ustundag, and M. Aslan, Comput. Mater. Sci. **98**, 136 (2015).
[7] R. P. Shahri and A. Akhtar, Chin. Phys. B **26**, 093107 (2017).
[8] M. Z. Hasan and J. E. Moore, Annu. Rev. Condens. Matter Phys. **2**, 55 (2011).
[9] P. Pyykko, Chem. Rev. **88**, 563 (1988).
[10] T. Jian, G. V. Lopez, and L. S. Wang, J. Phys. Chem. B **120**, 1635 (2016).
[11] T. Jian, L. F. Cheung, T. T. Chen, and L. S. Wang, Angew. Chem., Int. Ed. **56**, 9551 (2017).
[12] L. F. Cheung, J. Czekner, G. S. Kocheril, and L. S. Wang, J. Chem. Phys. **150**, 064304 (2019).

[13]W. J. Chen, M. Kulichenko, H. W. Choi, J. Cavanagh, D. F. Yuan, A. I. Boldyrev, and L. S. Wang, J. Phys. Chem. A **125**, 6751 (2021).
[14]H. Kim, X. Li, L. S. Wang, H. L. de Clercq, C. A. Fancher, O. C. Thomas, and K. H. Bowen, J. Phys. Chem. A **105**, 5709 (2001).
[15]I. Leon, Z. Yang, and L. S. Wang, J. Chem. Phys. **138**, 184304 (2013).
[16]J. Fan and L. S. Wang, J. Chem. Phys. **102**, 8714 (1995).
[17]J. B. Kim, M. L. Weichman, and D. M. Neumark, Mol. Phys. **113**, 2105 (2015).
[18]G. S. Kocheril, H. W. Gao, D. F. Yuan, and L. S. Wang, J. Chem. Phys. **157**, 171101 (2022).
[19]G. S. Kocheril, H. W. Gao, and L. S. Wang, Mol. Phys. **158**, 236101 (2023).
[20]G. S. Kocheril, H. W. Gao, and L. S. Wang, J. Chem. Phys. **158**, 236101 (2023).
[21]H. Gómez, T. R. Taylor, Y. Zhao, and D. M. Neumark, J. Chem. Phys. **117**, 8644 (2002).
[22]J. Ho, M. L. Polak, and W. C. Lineberger, J. Chem. Phys. **96**, 144 (1992).
[23]L. S. Wang, H. Cheng, and J. Fan, J. Chem. Phys. **102**, 9480 (1995).
[24]L. S. Wang, Int. Rev. Phys. Chem. **35**, 69 (2016).
[25]I. León, Z. Yang, H. T. Liu, and L. S. Wang, Rev. Sci. Instrum. **85**, 083106 (2014).
[26]B. Dick, Phys. Chem. Chem. Phys. **21**, 19499 (2019).
[27]J. Cooper and R. N. Zare, J. Chem. Phys. **48**, 942 (1968).
[28]A. Sanov and R. Mabbs, Int. Rev. Phys. Chem. **27**, 53 (2008).
[29]E. P. Wigner, Phys. Rev. **73**, 1002 (1948).
[30]H. Lefebvre-Brion and R. W. Field, *The Spectra and Dynamics of Diatomic Molecules* (Elsevier, Boston, 2004).
[31]C. Hock, J. B. Kim, M. L. Weichman, T. I. Yacovitch, and D. M. Neumark, J. Chem. Phys. **137**, 244201 (2012).
[32]M. L. Weichman and D. M. Neumark, Annu. Rev. Phys. Chem. **69**, 101 (2018).
[33]J. L. Gardner and J. A. R. Samson, J. Chem. Phys. **62**, 1447 (1975).